Journal of Alloys and Compounds 515 (2012) 68–73

Contents lists available at SciVerse ScienceDirect

Journal of Alloys and Compounds

journal homepage: www.elsevier.com/locate/jallcom

Effect of heat treatment on microstructures and mechanical behavior of porous Sr–Ca–P coatings on titanium

Kuan-Chen Kung[a], Kuo Yuan[b], Tzer-Min Lee[b,c,*], Truan-Sheng Lui[a]

[a] Department of Materials Science and Engineering, National Cheng Kung University, Tainan, Taiwan
[b] Institute of Oral Medicine, National Cheng Kung University, Tainan, Taiwan
[c] Medical Device Innovation Center, National Cheng Kung University, Tainan, Taiwan

ARTICLE INFO

Article history:
Received 15 September 2011
Received in revised form 2 November 2011
Accepted 11 November 2011
Available online 22 November 2011

Keywords:
Micro-arc oxidation (MAO)
Strontium
Heat treatment
Coatings
Mechanical properties

ABSTRACT

Titanium and its alloys are widely used in dental and orthopedic fields due to their excellent chemical stability. The micro-arc oxidation (MAO) technique is an effective method for coating strontium, calcium, and phosphorus onto titanium. In clinical application, the adhesion between the coating and the substrate is important factor for dental implants and artificial joint prosthesis. The present study investigates the effects of heat treatment on the properties of MAO coatings. The physicochemical characteristics are investigated using scanning electron microscopy (SEM) observation, thin film X-ray diffraction (TF-XRD) analysis, and the scratch test. After heat treatment, the TF-XRD results indicate that the tricalcium phosphate phase appears at a temperature of 800 °C. SEM results show that the surface morphology does not change. The scratch test results reveal that the adhesion strength between the coatings and the substrate increases with increasing heat treatment temperature. Consequently, all findings in this study indicated that MAO coatings with heat treatment have good mechanical properties for clinical applications.

1. Introduction

Titanium and its alloys have excellent mechanical properties and low cyto-toxicity, and are thus widely used in orthopedic and dental implant applications. Because titanium and its alloys are bio-inert, it is difficult to achieve a chemical bonding with bone tissue. In order to improve the bone-bonding ability of titanium, it is a good method that titanium substrates are coated with bioactive ceramics. Many modification techniques can be used to coat bioactive materials onto a titanium surface, such as plasma spraying [1], radio frequency (RF)-sputtering [2], and electrochemical techniques [3]. For example, titanium-alloy implants with plasma-sprayed hydroxyapatite (HA) coatings have been shown the direct physicochemical bone bonding and reliable interface strength to surrounding bone tissue. However, high-temperature processing of plasma-spraying has several drawbacks, including poor adhesion between the coating layer and metal substrate, difficulties in controlling the composition, and in using for complex surface geometries, such as dental implants with screw. Some clinical studies indicated that the long-term performance of implants with plasma-sprayed coatings is not better than that of uncoated implants [4].

A calcium phosphate ceramic coating on a titanium implant surface forms a direct and strong bonding with bone and is more rapidly integrated than metals during the early stage after implantation. It is noticed that strontium (Sr), which increases bone formation and reduces bone resorption, is beneficial for biological applications for bone regeneration [5]. Recently, the strontium-substituted calcium phosphates have been developed [6]. Strontium-substituted calcium phosphate coatings can improve fixation and extend lifetime of the implant. However, strontium-substituted calcium phosphate ceramics have insufficient mechanical strength to be used in load-bearing applications. The excellent biocompatibility and bioactivity of ceramics and the good mechanical properties of titanium and its alloys can be combined using modification techniques.

A particular electrochemical technique, the micro-arc oxidation (MAO, also called as anodic spark oxidation or micro-arc discharge oxidation) process is an effective technique for forming oxide coatings on metal surfaces such as aluminum, magnesium, zirconium, and titanium. This method combines the chemical and morphological modification of titanium surfaces in a single process step, and allows coatings properties such as oxide thickness, chemical composition, pore size, and roughness to be easily controlled. Besides, an advantage of MAO method is to form uniformly porous oxide coatings on implant surfaces with complex geometries. However, it

* Corresponding author at: Institute of Oral Medicine, National Cheng Kung University, Tainan, Taiwan. Tel.: +886 6 2353535x5972; fax: +886 6 2359885.
E-mail address: tmlee@mail.ncku.edu.tw (T.-M. Lee).

0925-8388/$ – see front matter © 2011 Elsevier B.V. All rights reserved.
doi:10.1016/j.jallcom.2011.11.050

Table 1
Composition of MAO electrolyte.

Specimen	Solution composition (M)		
	$NaH_2PO_4 \cdot H_2O$	$Ca(CH_3COO)_2 \cdot H_2O$	$Sr(OH)_2 \cdot 8H_2O$
CP	0.06	0.13	0
CPS1	0.06	0.1287	0.0013
CPS5	0.06	0.1235	0.0065
CPS10	0.06	0.117	0.013

has been recognized that MAO coatings containing strontium have an amorphous phase [7]. An appropriate thermal treatment could enhance crystallization because amorphous calcium phosphate is thermodynamically metastable [8]. It has been suggested that the mechanical properties of MAO coatings containing strontium could be improved by heat treatment.

In the present study, MAO was used to modify a titanium surface in aqueous electrolyte, allowing strontium, calcium, and phosphorus to be incorporated into a titanium oxide matrix in a single anodic oxidation reaction. Heat treatment was used to modify the microstructure, crystallinity, phase, and mechanical properties of MAO coatings. The MAO coating microstructure was observed by scanning electron microscopy (SEM). The crystallinity and phase of the MAO coatings were identified using thin-film X-ray diffraction (TF-XRD). The scratch test method was used to evaluate the mechanical properties.

2. Materials and methods

2.1. Preparation of specimens and post-heat treatment

Medical grade titanium (commercially pure Ti, Grade 2, ASTM F-67) was selected as the substrate. The dimension of the titanium disk was 12.7 mm in diameter and 2 mm in thickness. The substrates were ground using silicon carbide papers from 320-, 400-, 600-, 800-, 1000-, 1200-, 1500-grit, in sequence, and then ultrasonically cleaned in acetone, ethanol, and de-ionized water prior to micro-arc oxidation. Four kinds of electrolyte were applied to modify the composition of MAO coatings. The MAO electrolyte was prepared by dissolving sodium phosphate monobasic monohydrate ($NaH_2PO_4 \cdot H_2O$), calcium acetate hydrate ($Ca(CH_3COO)_2 \cdot H_2O$), and strontium hydroxide 8-hydrate ($Sr(OH)_2 \cdot 8H_2O$) in de-ionized water.

For MAO treatment, the specimens were anodized with a DC power supply (GPS-60H15S, GW). The specimen was used as the anode, and a stainless steel plate was used as the cathode in the electrochemical cell. The samples were treated with an applied voltage of 350 V for 1 min. The electrolyte temperature was cooled by a circulating water system to keep the temperature at 25 °C. After MAO treatment, the samples were sequentially rinsed with acetone, ethanol, and de-ionized water, and then dried in an oven. By adjusting the strontium content in the electrolyte, four kinds of MAO coating were prepared. As shown in Table 1, the MAO specimens are denoted as CP, CPS1, CPS5, and CPS10 in accordance with the preparation of experimental materials formed by strontium content in electrolyte, respectively. The characteristics of the MAO coatings are summarized in Table 2 [7]. For heat treatment, the specimens were heated at temperatures of 400–800 °C, respectively with a heating rate of 5 °C min^{-1} and then held for 2 h.

2.2. Materials characterization

After heat treatment, the MAO coatings phase was identified by TF-XRD (Rigaku D/max III. V) with a scan speed of 4° min^{-1} between 20 and 60 (2θ angle), using Cu-Kα radiation. The surface morphology of the specimens was observed by SEM (JEOL JSM-6390LV).

Table 2
Elemental composition and thickness of MAO coatings [7].

Specimen	EDX results (wt%)					Thickness
	Ti	O	Ca	P	Sr	(μm)
CP	45.02	48.36	3.69	2.93	0	3.72
CPS1	45.18	48.13	3.67	2.87	0.15	3.70
CPS5	45.21	48.03	3.40	2.81	0.55	3.79
CPS10	45.47	47.85	3.19	2.55	0.94	3.74

2.3. Mechanical property test

The scratch test was used to evaluate the adhesion between the coating and the substrate. The mechanical strength of adhesion between the MAO coatings and the substrate was measured using the scratch test (MFT-4000) with a 200-μm radius diamond indenter. Three specimens were utilized for the determination of adhesion strength. The load speed was 10 N min^{-1} and the scratch length was 4 mm. The datasets were processed using proprietary software to produce load-displacement curves. The adhesion strength was calculated from the slopes of the curves. After the scratch test, the scratch morphology was observed by SEM.

3. Results

3.1. Morphology of MAO coating surface

Fig. 1(a–f) shows SEM micrographs of the MAO CPS10 coatings after heat treatment at various temperatures. At low magnification, the rough and three-dimensional structures with open pores were observed in all as-prepared and heated specimens. These open pores are characteristically produced by the spark discharge in the MAO process. In comparison with as-prepared MAO CPS10 coatings, all specimens with heat treatment showed the same morphology. High-magnification morphologies of four MAO coatings after heat treatment at a temperature of 800 °C are shown in Fig. 2. There are visible microcracks in the MAO coatings and some precipitates were observed on the surface.

3.2. Phase identification

The phase of MAO coatings with heat treatment was characterized by TF-XRD analysis. Fig. 3 shows the XRD patterns of MAO CPS10 specimens before and after heat treatment at various temperatures (400–800 °C). Before heat treatment, three kinds of phase, namely the anatase (TiO_2), rutile (TiO_2), and titanium phases, were identified from the diffraction patterns, as shown in Fig. 3(a). The results indicate that the MAO coatings are mainly composed of the anatase structure containing rutile. During the MAO process, the electrolytes provided strontium, calcium, and phosphorus, which became incorporated into the TiO_2 matrix of the coatings.

After heat treatment, the intensity of the anatase and rutile phases became stronger, as shown in Fig. 3(b–f). The diffraction peaks of tricalcium phosphate ($Ca_3(PO_4)_2$) were detected on the surface of MAO coatings after heat treatment at a temperature of 800 °C. The results indicate that heat treatment enhances the crystallinity of TiO_2 (anatase and rutile) and induces the crystallization of the amorphous CaP. The XRD patterns for four kinds of MAO coating with heat treatment at various temperatures exhibited the same trends.

3.3. Scratch tests

The critical load values of MAO coatings with heat treatment at various temperatures are shown in Fig. 4. The values of critical load increased with increasing heat treatment temperature. The critical load of as-prepared CPS10 coatings was 11.3 N. The critical load of CPS10 specimens increased to 13.3, 16.2, 18.2, 19.4, and 21.4 N after heat treatment at temperature of 400, 500, 600, 700, and 800 °C, respectively. The results reveal that heat treatment improves the adhesion strength between the MAO coating and the titanium substrate.

Fig. 5 shows the whole track morphology of the scratch test of the MAO coatings. A typical image of a scratch indicates the location of penetration through the MAO coatings to the titanium substrate. The MAO coatings were extruded to both sides at the beginning of the track. Severe delamination and fractures can be seen in the coating. At the beginning of the track, the broad scratch width of the as-prepared MAO coating (Fig. 5(a)) was compared with those of

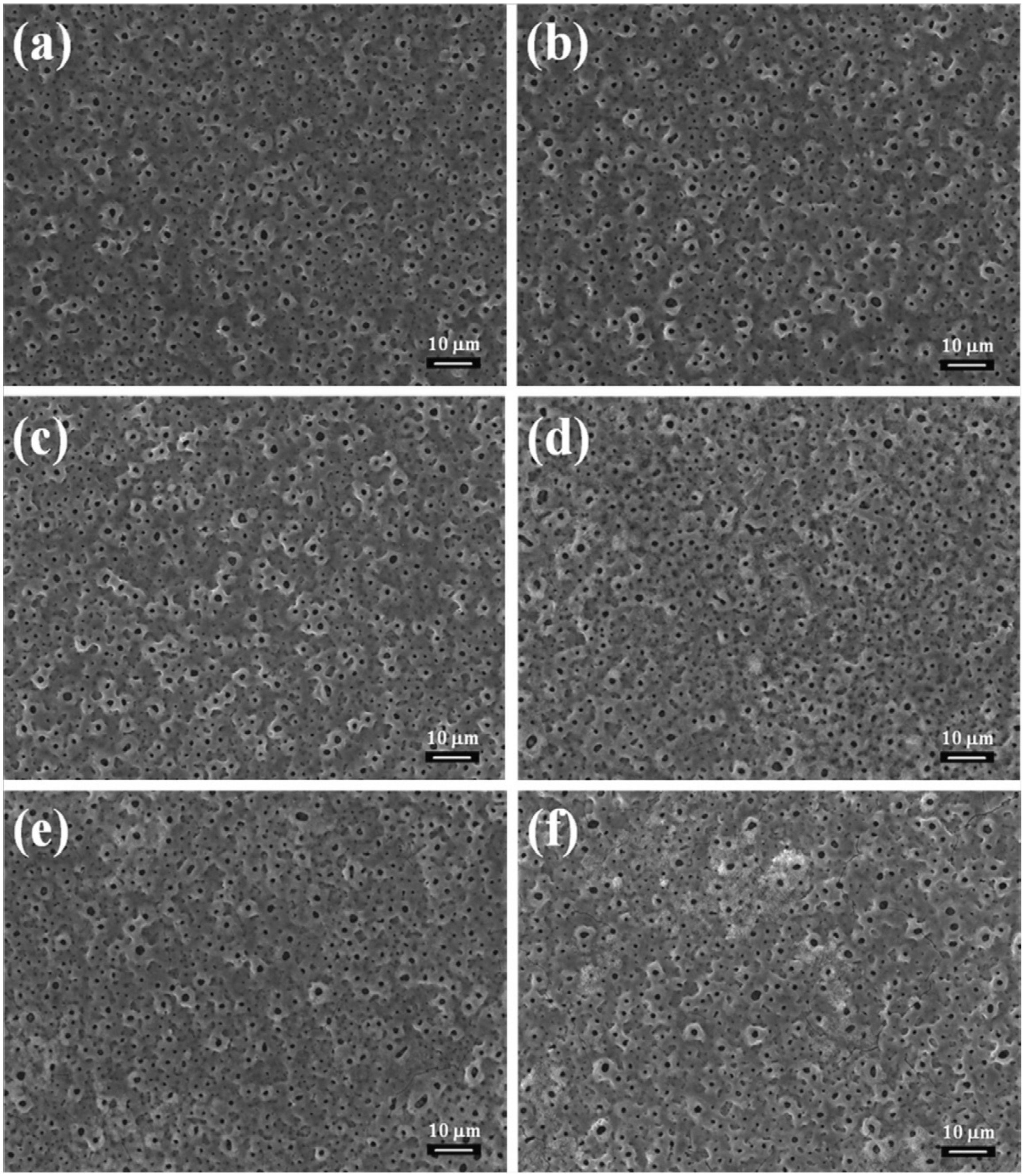

Fig. 1. Morphologies of (a) as-prepared MAO CPS10 coatings and MAO coatings heat treated at (b) 400 °C, (c) 500 °C, (d) 600 °C, (e) 700 °C, and (f) 800 °C.

other specimens. The width of the scratch decreased with increasing heat treatment temperature, indicating that the as-prepared MAO coating was ductile. At the end of the track, the MAO coatings with heat treatment at a temperature of 800 °C showed large fractures, which shows the brittleness of MAO coatings after heat treatment, especial at high temperature.

4. Discussion

There are many modification techniques for improving the biocompatibility of titanium implants. They change the structure, chemical composition, and morphology of the titanium surface. The MAO technique, which combines chemical composition and morphological modification in a single step, is a simple, controllable, and cost-effective method compared to other techniques such as plasma-spraying. The MAO process produces porous and uniform oxide coatings on implant surfaces with complex geometries, such as dental root implants. As shown in Fig. 1(a), the microstructure of the MAO coating has a uniform, porous, and three-dimensional structure. Table 2 indicates that the MAO electrolyte containing strontium, calcium, and phosphorus produced coatings with Sr–Ca–P embedded in the TiO_2 matrix. Choi et al. [9] investigated the formation of coatings on screw-shaped implants by applying various voltages. Their results revealed that the pore size, thickness, and roughness increased with increasing voltage, and the MAO surface morphology implant could introduce the more endosteal and periosteal bone formation in rabbit tibia.

As shown in Fig. 3(a), the titanium oxide matrix of as-prepared MAO CPS10 coatings consists of the anatase and rutile phases. Although the crystalline phase of strontium, calcium, and

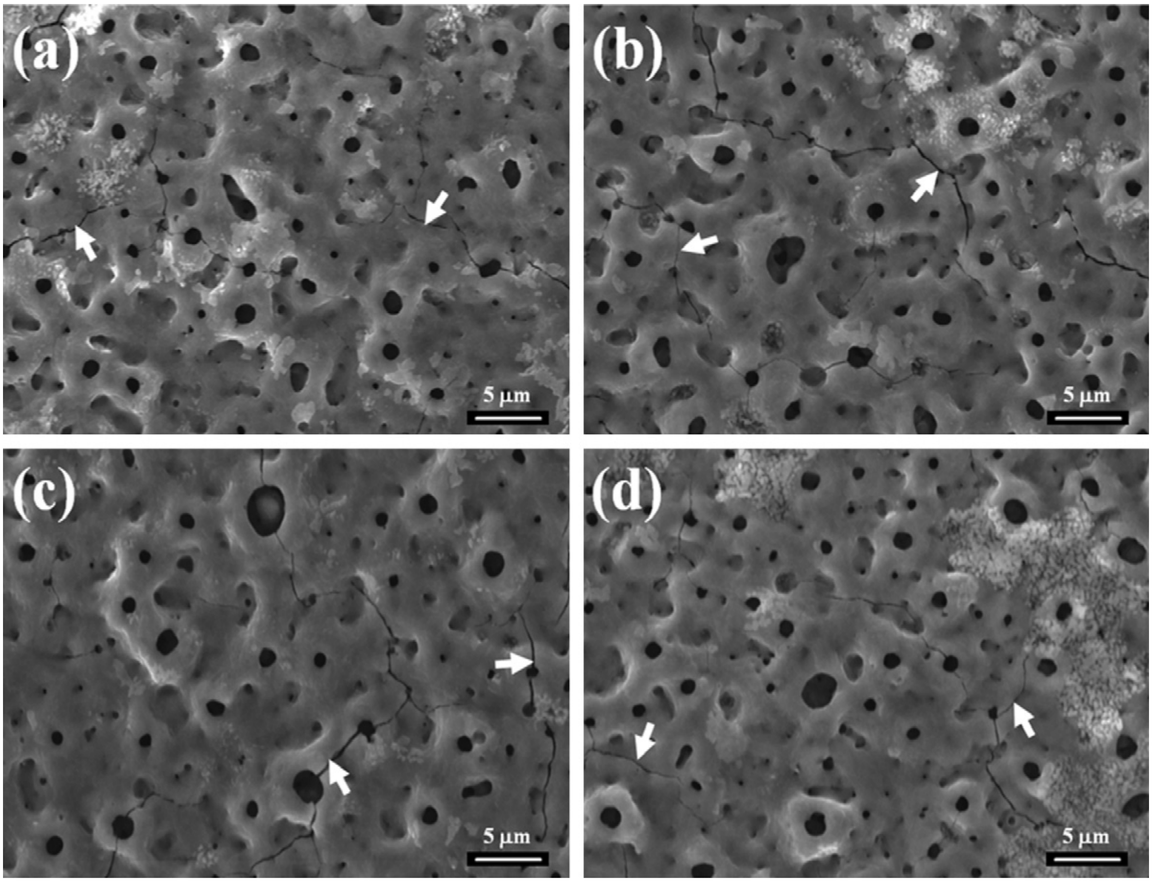

Fig. 2. High-resolution SEM micrographs of MAO coatings heat treated at 800 °C. (a) CP, (b) CPS1, (c) CPS5, and (d) CPS10.

phosphorus are undetectable in MAO coatings by TF-XRD, it can be inferred that the titanium oxide composition contained the Sr–Ca–P–O amorphous phase [7]. Similar results were obtained in other studies [10,11]. Han et al. indicated that the MAO coating was a mixture of the rutile and anatase phases at high voltage [11]. The MAO coating only consisted of the anatase phase at low voltage. An appropriate thermal treatment can induce new phase formation and improve crystallinity. In this study, heat treatment affected the structural properties, such as phase composition and crystallinity of TiO_2, of MAO coatings. The morphologies of MAO coatings with heat treatment at various temperatures are shown in Fig. 1(b–f). Some precipitates can be observed on the surface of the MAO coatings, as shown in Fig. 1(f). TF-XRD diffraction peaks of tricalcium phosphate ($Ca_3(PO_4)_2$) appear for the MAO coating surface after heat treatment at a temperature of 800 °C, as shown in Fig. 3(f). This may be attributed to the heat treatment leading to crystallization and new phase formation in the MAO coating [12]. The intensities of the anatase and rutile phases increased with increasing heat treatment temperature. Moreover, the MAO electrolyte provides strontium, calcium, and phosphorus, which become incorporated into the TiO_2 matrix of the coatings. As shown in Fig. 2, the number of microcracks increases with increasing heat treatment temperature. Due to the thermal expansion of MAO coating,

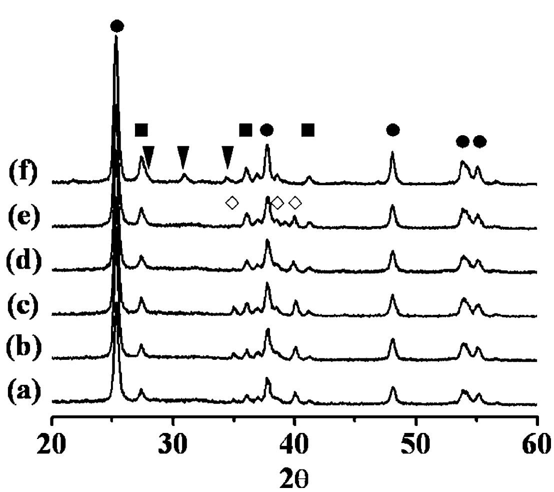

Fig. 3. TF-XRD patterns of (a) as-prepared CPS10 specimens and CPS10 specimens heat treated at (b) 400 °C, (c) 500 °C, (d) 600 °C, (e) 700 °C, and (f) 800 °C. (●: anatase; ■: rutile; □: titanium; ▼: $Ca_3(PO_4)_2$).

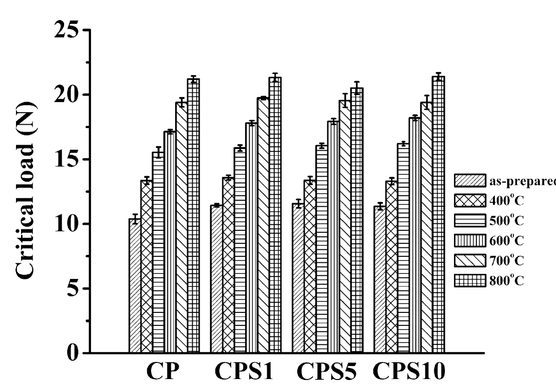

Fig. 4. Critical load in scratch test for MAO coatings with heat treatment at various temperatures.

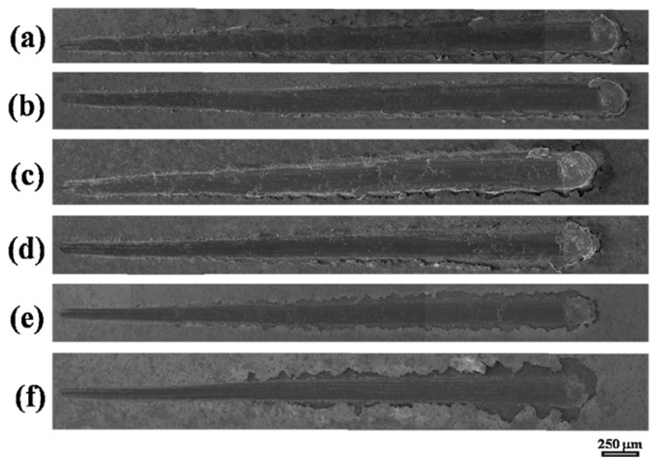

Fig. 5. Whole track morphologies from scratch test of (a) as-prepared CPS10 specimens and CPS10 specimens heat treated at (b) 400 °C, (c) 500 °C, (d) 600 °C, (e) 700 °C, and (f) 800 °C.

there is a mismatch of the crystallization of composition phases [13]. Goueffon et al. [14] reported that the thermal cycling of black anodized aluminum alloy enhances cracks and decreases adhesion of the coating due to the difference in the coefficient of thermal expansion between the coating and the substrate.

After heat treatment, the increased rutile phase and tricalcium phosphate phase were observed, as shown in Fig. 3. The two kinds of phases could improve the properties of the MAO coatings. For example, the rutile possesses much better protective property [15] and more stable than anatase phase [16]. Other study indicated that the titanium was modified by MAO treatment and sequentially was subjected to heat treatment at 600 °C [17]. Because only the phase of rutile was formed by heat treatment, it could induce precipitations of bone-like apatite in the stimulated body fluid. Saldaña et al. [18] revealed that the rutile could improve the *in vitro* biocompatibility, in terms of initial cell attachment, alkaline phosphatase (ALP) secretion, and osteoprotegerin (OPG) secretion. Furthermore, tricalcium phosphate has been widely used in dentistry and orthopedics due to their excellent biological properties such as osteoconduction [19]. Ohgushi et al. [20] showed that the bone formation ability of tricalcium phosphate implants was similar to hydroxyapatite implants after implantation for two months. Moreover, the ALP/DNA ratio of tricalcium phosphate substrates was higher compared to other substrates of PLLA, PC, and glass which indicated that tricalcium phosphate substrates enhance bone mineralization [21]. The results suggested that the phase formation of rutile and tricalcium phosphate was benefit to biological properties.

MAO coatings on titanium implants are used in load-bearing applications in the clinic. Due to the poor adhesion strength of the coatings, the coating can become separated from the substrate. Good mechanical performance is very important for dental implants. It has been reported that the fracture site of plasma-sprayed HA coating moves from the bone-coating interface to the coating-substrate interface with increasing time [22]. Therefore, the adhesion strength between the coating and substrate is a key mechanical property. In this study, the critical load of as-prepared and heated MAO coatings ranged from 10.4 N to 21.4 N (Fig. 4). Rohanizadeh et al. [23] deposited an apatite coating onto titanium using chemical deposition. The coating adhesion was measured using the scratch test to be about 13.1 N. The HA coating, which was prepared using electrochemical deposition, was scraped off from the titanium substrate at a load of 20 N [3]. A study [24] synthesized HA powder via a wet method using $Ca(NO_3)_2$ and $(NH_4)_2HPO_4$ and then used the powder to form a suspension with water and alcohol. An HA coating was then deposited onto titanium using plasma spraying technique. The adhesion strength of the HA coatings to the substrate was 10–12 N, as obtained from the scratch test. Arias et al. [25] reported that a thin film of calcium phosphate coated onto titanium by pulsed-laser deposition was partially removed (revealing the substrate) at 9.6 N. In the present study, heat treatment improved the adhesion strength between the MAO coating and the titanium substrate.

The results of the scratch test are a function of the coating thickness, ductility, shape, and brittleness [23]. Some studies reported that the thickness of coatings significantly influences the mechanical properties [26]. For example, the mean critical load increased with increasing thickness of a coating prepared by anodization [27]. Chen et al. [28] reported that the 20-μm thick MAO TiO_2 coatings, whose critical load in the scratch test was about 36 N, showed a high adhesion strength. As shown in Table 2, the average thickness of four kinds of MAO coating was 3.7 μm. The critical load in the scratch test was about 11 N. This result indicates that there was excellent adhesion strength between the MAO coating and the substrate. Moreover, a crystalline amorphous coating, which was prepared by pulsed-laser deposition on a substrate maintained at 460 °C, deforms plastically without detaching from the substrate [25]. As shown in Fig. 5, fractures were observed for the scratch track with high-temperature heat treatment. This reveals that the MAO coatings became brittle after high-temperature heat treatment. Fig. 4 shows the critical load in the scratch test for the MAO coatings with heat treatment at various temperatures. The critical load value for the MAO coatings with heat treatment at a temperature of 800 °C is 2-fold that of the as-prepared MAO coatings. The results show that the MAO coatings with heat treatment had improved adhesion strength. Ishizawa et al. [29] reported that the push-out strengths of anodic amorphous calcium phosphate oxide films on titanium were lower than those for hydrothermally treated films after 8 weeks of implantation in rabbit femurs.

In this study, strontium, which simulates bone formation and decreases bone resorption, was incorporated into the MAO coatings. As shown in Fig. 4, the adhesion strength increased with increasing heat treatment temperature. This suggests that heat treatment improved the mechanical properties. However, the critical load value did not differ significantly between the heat-treated MAO coatings containing different contents of strontium, as shown in Fig. 4. The whole track morphologies of the four kinds of MAO coatings with heat treatment at various temperatures show the same trend. The results reveal that the strontium in the MAO coatings did not affect the adhesion strength. Therefore, excellent adhesion strength of the MAO coatings can be attributed to heat treatment. The increased rutile phase and new phase of tricalcium phosphate were benefit to biological responses. Further studies will have to be performed to confirm the effect of heat treatment on the biological performance of the MAO coatings, such as bioactivity and biological properties.

5. Conclusions

The coatings containing strontium, calcium, and phosphorus with a uniform and porous structure were fabricated using the MAO technique. The effects of heat treatment on the microstructure and adhesion strength of MAO coatings were characterized using SEM, TF-XRD, and the scratch test. The following results were obtained:

(1) The surface morphologies of the MAO coatings did not change after heat treatment. TF-XRD patterns show that the crystallinity of the anatase and rutile phases increased with increasing heat treatment temperature. Moreover, the tricalcium

phosphate ($Ca_3(PO_4)_2$) phase was observed after heat treatment at 800 °C.

(2) Due to the thermal expansion mismatch between the MAO coatings and the titanium substrate, large fractures were observed after heat treatment at 800 °C.

(3) The adhesion strength of the MAO coatings increased with increasing heat treatment temperature. The existence of strontium in the MAO coatings did not alter the mechanical strength compared to Sr-free MAO coatings.

All measurements indicate that the mechanical properties and crystallinity of MAO coatings are improved after heat treatment. Heat treatment at an optimal temperature can enhance adhesion performance of MAO coatings for medical applications.

Acknowledgments

The work was financially supported by the National Science Council of Taiwan under grant NSC 99-2221-E-006-093.

References

[1] C.Y. Yang, T.M. Lee, C.W. Yang, L.R. Chen, M.C. Wu, T.S. Lui, J. Biomed. Mater. Res. 83A (2007) 263–271.
[2] J.G.C. Wolke, J.P.C.M. van der Waerden, H.G. Schaeken, J.A. Jansen, Biomaterials 24 (2003) 2623–2629.
[3] M.C. Kuo, S.K. Yen, Mater. Sci. Eng. C 20 (2002) 153–160.
[4] H.H. Liao, B. Fartash, J.G. Li, Clin. Oral Implan. Res. 8 (1997) 68–72.
[5] P.J. Meunier, C. Roux, E. Seeman, S. Ortolani, J.E. Badurski, T.D. Spector, J. Cannata, A. Balogh, E.-M. Lemmel, S. Pors-Nielsen, R. Rizzoli, H.K. Genant, J.-Y. Reginster, N. Engl. J. Med. 350 (2004) 459–468.
[6] M.D. O'Donnell, Y. Fredholm, A. De Rouffignac, R.G. Hill, Acta Biomater. 4 (2008) 1455–1464.
[7] K.C. Kung, T.M. Lee, J.L. Chen, T.S. Lui, Surf. Coat. Technol. 205 (2010) 1714–1722.
[8] C.W. Yang, T.M. Lee, T.S. Lui, E. Chang, Mater. Sci. Eng. C 26 (2006) 1395–1400.
[9] J.W. Choi, S.J. Heo, J.Y. Koak, S.K. Kim, Y.J. Lim, S.H. Kim, J.B. Lee, J. Oral Rehabil. 33 (2006) 889–897.
[10] H. Ishizawa, M. Ogino, J. Biomed. Mater. Res. 29 (1995) 65–72.
[11] Y. Han, S.H. Hong, K.W. Xu, Surf. Coat. Technol. 168 (2003) 249–258.
[12] F.Y. Jin, P.K. Chu, K. Wang, J. Zhao, A.P. Huang, H.H. Tong, Mater. Sci. Eng. A 476 (2008) 78–82.
[13] D.Q. Wei, Y. Zhou, D.C. Jia, Y.M. Wang, Surf. Coat. Technol. 201 (2007) 8723–8729.
[14] Y. Goueffon, L. Arurault, C. Mabru, C. Tonon, P. Guigue, J. Mater. Process. Technol. 209 (2009) 5145–5151.
[15] A.L. Yerokhin, X. Nie, A. Leyland, A. Matthews, Surf. Coat. Technol. 130 (2000) 195–206.
[16] L.H. Li, Y.M. Kong, H.W. Kim, Y.W. Kim, H.E. Kim, S.J. Heo, J.Y. Koak, Biomaterials 25 (2004) 2867–2875.
[17] B.C. Yang, M. Uchida, H.M. Kim, X.D. Zhang, T. Kokubo, Biomaterials 25 (2004) 1003–1010.
[18] L. Saldaña, N. Vilaboa, G. Vallés, J. González, L. Munuera, J. Biomed. Mater. Res. 73A (2005) 97–107.
[19] W.C. Xue, J.L. Moore, H.L. Hosick, S. Bose, A. Bandyopadhyay, W.W. Lu, M.C. Kenneth, Cheung, D.K. Luk Keith, J. Biomed. Mater. Res. 79A (2006) 804–814.
[20] H. Ohgushi, M. Okumura, S. Tamai, E.C. Shors, A.I. Caplan, J. Biomed. Mater. Res. 24 (1990) 1563–1570.
[21] Y. Yang, J. Magnay, L. Cooling, J.J. Cooper, A.J. El Haj, Med. Biol. Eng. Comput. 42 (2004) 22–29.
[22] K. Hayashi, T. Inadome, T. Mashima, Y. Sugioka, J. Biomed. Mater. Res. 27 (1993) 557–563.
[23] R. Rohanizadeh, R.Z. LeGeros, M. Harsono, A. Bendavid, J. Biomed. Mater. Res. 72A (2005) 428–438.
[24] L. Łatka, L. Pawlowski, D. Chicot, C. Pierlot, F. Petit, Surf. Coat. Technol. 205 (2010) 954–960.
[25] J.L. Arias, M.B. Mayor, J. Pou, Y. Leng, B. León, M. Pérez-Amor, Biomaterials 24 (2003) 3403–3408.
[26] X. Nie, A. Leyland, H.W. Song, A.L. Yerokhin, S.J. Dowey, A. Matthews, Surf. Coat. Technol. 116–119 (1999) 1055–1060.
[27] J. Blackwood Daniel, W. Seah Kar Heng, J. Biomed. Mater. Res. 93A (2010) 1551–1556.
[28] C.Z. Chen, Q. Dong, H.J. Yu, X.B. Wang, D.G. Wang, Adv. Eng. Mater. 8 (2006) 754–759.
[29] H. Ishizawa, M. Fujino, M. Ogino, J. Biomed. Mater. Res. 29 (1995) 1459–1468.